International Journal of Reconfigurable and Embedded Systems (IJRES)
Vol. 14, No. 3, November 2025, pp. 717~724
ISSN: 2089-4864, DOI: 10.11591/ijres.v14.i3.pp717-724

The impacts of optical display BaF_2-Ce materials on solid-state lighting

Luu Hong Quan[1], Nguyen Thi Phuong Loan[2]
[1]Faculty of Electrical and Electronics Engineering, HCMC University of Industry and Trade, Ho Chi Minh City, Vietnam
[2]Faculty of Fundamental 2, Posts and Telecommunications Institute of Technology, Ho Chi Minh City, Vietnam

Article Info

Article history:

Received Jan 7, 2025
Revised Aug 17, 2025
Accepted Oct 9, 2025

Keywords:

BaF_2-Ce
Color quality scale
Color rendering index
Lambert-Beer law
Luminous efficacy
White light-emitting diode

ABSTRACT

Transparent ceramic doped with barium fluorid cerium (BaF_2-Ce) was created via a sintering method and its brightness and scintillation characteristics were examined. The luminescence is associated with the 5d-4f transitions in the Ce^{3+} ion and exhibits emitting maxima at 310 and 323 nm. For Na-22 radioisotopes, photo-maximum at 511 keV and 1274 keV were achieved using translucent ceramic BaF_2-Ce. The translucent ceramic BaF_2-Ce has been determined to have a power resolution of 13.5% at 662 keV. A luminescent production rate was measured for the BaF_2-Ce (0.2%) ceramic, which is similar to sole crystal. Calculations of the scintillation degradation period beneath 662 keV gamma stimulation reveal a quick part of 58 ns and a somewhat sluggish part of 434 ns. The more gradual part in BaF_2-Ce(0.2%) ceramic is linked to the dipole-dipole power transmission from the host structure to the Ce^{3+} luminous core and is quicker comparing to self-trapped excitons (STE) emitting in BaF_2 host. BaF_2-Ce offer various qualities, including significant illumination output, rapid degradation duration, and rapid scintillating reaction, which are desirable for many global fields such as medicine, radiation detection, industrial systems and nuclear safety.

Corresponding Author:

Luu Hong Quan
Faculty of Electrical and Electronics Engineering, HCMC University of Industry and Trade
Ho Chi Minh City, Vietnam
Email: quanlh@huit.edu.vn

1. INTRODUCTION

A scintillator for gamma ray spectroscopy must have a strong illumination production, an elevated density and a quick degradation time [1]-[4]. Organic scintillators are not as good as sole crystal scintillators because of their lower power resolution and higher density. Inorganic sole crystals are costly because they are hard to generate in huge quantities, notwithstanding the potential of inorganic scintillators like $LaBr_3$-Ce [5]. Translucent polycrystalline ceramics are currently a more affordable option than sole crystals [6], [7]. Translucent polycrystalline ceramics are reasonably priced, easily fabricated in high volumes, and are capable of being uniformly and extensively doped with active ions [8]-[10]. In the first place, compared to sole crystals, ceramics are often stronger in mechanics. The opaque nature of conventional ceramics was a disadvantage for scintillation applications [11]. Nevertheless, because of the advancements in nanotechnology and sintering process, ceramics' optic transparent nature has greatly increased, opening the door for scintillation uses [12]. In addition to scintillation, they can also be utilized for detecting high-energy particles, time-of-flight positron emission tomography (TOF-PET) scanners, Xray and gamma ray visualization, as well as radiation detectors.

One term for clean barium fluoride (BaF_2) is rapid scintillator. A sole crystal of BaF_2 displays two emitting ranges. Self-trapped excitons (STE) production is rather gradual, reaching the maximum at 310 nm with a degradation period of 630 ns, while the rapid part is in the ultraviolet (UV) area of about 195-220 nm having a degradation period ranging from 600-800 ps [13]-[15]. The quick part produces just 15% of the photoelectrons, whereas the more gradual part accounts for 85% of the degeneration [16]. BaF_2's sluggish emitting has been suppressed and its duration resolution has been improved by the application of multiple uncommon earth doping techniques [1], [2], [17], [18]. Nevertheless, the process led to the quenching of the rapid and gradual production [16]. A different approach method is to use Ce^{3+} doping to convert the more gradual STE generation into the faster Ce^{3+} generation. Prior research was conducted on Ce^{3+} doped BaF_2 crystal. Using BaF_2-Ce^{3+} crystals as a case study, My *et al.* [15] demonstrated rapid Ce^{3+} generation beneath X-ray stimulation, having the greatest strength for Ce^{3+} concentrations of roughly 0.2 mol%. The scintillation characteristics and degradation period of Ce^{3+} doped BaF_2 crystals having the lowering of sluggish BaF_2 generation have been described by Tung *et al.* [3], Cong *et al.* [4]. On the optic and scintillating characteristics of Ce^{3+} doped BaF_2 ceramics, yet, not many investigations have been published [5], [6]. Furthermore, there is no information regarding the creation of a photo-maximum using translucent ceramic BaF_2-Ce. It is important for investigating the scintillating characteristics of BaF_2-Ce ceramics owing to the increasing attention on ceramic scintillators. Throughout this work, we created a BaF_2 ceramic doped with 0.2 mol% Ce^{3+} that was roughly Ø 10×1 mm^2 and examined its luminous and scintillating characteristics. Regarding Na-22 and Cs-137 radioisotopes, the pulse height hue ranges collected from BaF_2-Ce translucent ceramic exhibit a photo-maximum with a full-width half maximum (FWHM) power resolution of 13.5% at 662 keV.

2. RESEARCH METHOD

2.1. BaF_2-Ce(0.2%) translucent ceramic creation

The $Ba(NO_3)_2$ and kalium fluorida (KF) mixture were produced in a $Ce_{0.001}Ba_{0.999}F_{2.001}$ proportion with deionized water being the solvent. $Ce(NO_3)_3{\cdot}6H_2O$ and PEG2000 were mixed together in a $Ba(NO_3)_2$. The KF compounds were added to the combined compound. Following the end of the precipitating procedure, the combined compound was left over 24 hours. The precipitating results were rinsed with deionized water and filtered. The precipitating results were subsequently left to dry during 24 hours. The dried powders were crushed and compacted into 10×5 mm discs using 200 MPa uniaxial pressures. The compacts were subjected to cold isostatic pressure and sintered in the vacuum sealed furnace (VSF) and a temperature rise of 10 ºC per minute. The furnace container is composed of elevated-heat stainless steel, while the inside container is built of fiber graphite. The thermal component is composed of SieMo. The sintering heat was initially set at 1000 ºC during 2 hours, and subsequently increased to 1300 ºC during the following 6 hours. The sintered specimens were taken for grinding and polished.

2.2. Characterization

The phase structure of BaF_2-Ce has been investigated utilizing a Bruker D8 ADVANCE X-ray diffractometer. PL and PLE have been determined using an Edinburgh FS5 spectrofluorometer. The specimen's production was studied utilizing the X-ray-generated optic luminosity (XEOL) method. The scintillating reaction to gamma 662 KeV and 511 KeV was determined with a superior bi-alkali Hamamatsu photomultiplier tube (PMT). The PMT production was processed using Hamamatsu preamplifier and shaped using a spectroscopic Ortec amplifier. The multi-channel analysis device was a Canberra MPII. Scintillating period was calculated utilizing gamma stimulation and PMT, with the preamplifier emission seen on a Picotech digital oscilloscope. The deterioration period was calculated using exponential fitting of the results of experiments. Luminous yield (LY) is estimated by comparing the region beneath the pulse period graph to the same pulse recorded with a NaI(Tl) luminescent material beneath the same circumstances.

3. RESULTS AND DISCUSSION

We now discuss the XRD structure of BaF_2-Ce(0.2%) nanoparticles and translucent ceramic. The whole maxima connect to the clean cubic stage of BaF_2-Ce. The nanoparticles and ceramic specimens do not contain any subsequent stages. The luminescence emitting and stimulation hue range of BaF_2-Ce(0.2%) are presented. The luminescence stimulation (PLE) hue range has the highest point at 300 nm and another at approximately 280 nm. BaF_2-Ce(0.2%) emits at 310 and 323 nm when stimulated with 279 and 300 nm, respectively. In contrast to clean BaF_2, BaF_2-Ce ceramic lacks a rapid element having a maximum at 195-220 nm. The light emitted at 310 nm overlaps over the STE generation in clean BaF_2. Ce^{3+} doped fluorides scintillators emit at 310 and 323 nm due to transfers from the 5d range's underneath to the $^2F_{5/2}$ and

$^2F_{7/2}$ power values of the Ce^{3+} ions' $4f^1$ arrangement [4], [5], [19]-[22]. We studied the light emission of BaF_2-Ce using XEOL. XEOL offers the benefit of detecting every generation in a specimen. According to XEOL, X-rays penetrate the material to generate charge carriers that may remix and create illumination. The XEOL spectra produced using an X-ray stimulation reveals generations 310-323 nm in BaF_2-Ce, but the clean BaF_2's rapid part is suppressed. Ce-doping in BaF_2-Ce ceramics causes a decrease in rapid BaF_2 generation, which differs in comparison to the less rapid STE generation of clean BaF_2.

For better comprehension of the source generations in BaF_2-Ce, the scintillating degradation period was determined by using gamma stimulation. Scintillation degradation periods were computed using exponential matching of result from experiments. Scintillation degradation studies show a bi-exponential deterioration, which has a quick part that is 58 ns and strength of 37%, and a more gradual part of 434 ns having strength of 63%. The degradation periods measured are close to those published for Ce^{3+} doped BaF_2 sole crystals [4]. The rapid part is attributed to the Ce^{3+} ion's 5d-4f transformation. The degradation period is common for Ce^{3+} illumination in various settings [5], [15], [20], [22], [23]. The more gradual degradation part is less lengthy than STE production in BaF_2 host. Furthermore, the more slowly element strength (63%) in BaF_2-Ce is reduced in comparison to 85% in clean BaF_2, as described. The less lengthy degradation period of 434 ns in BaF_2-Ce as opposed to roughly 630 ns in clean BaF_2 could be attributed to dipole-dipole power transmission from the host network to the Ce^{3+} luminescent core. Dipole-dipole power transmission from the donor (BaF_2) to a receiver (Ce^{3+}) reduces the donor's luminous strength and degradation [24], [25]. In (1) [25], [26] relates the effectiveness of dipole-dipole power transmission (E) to the degradation period of the donor (BaF_2 host network).

$$E = 1 - \frac{\tau_{DA}}{\tau_D} = 1 - \frac{F_{DA}}{F_D} \quad (1)$$

τ_{DA} and τ_D represent the donor's degradation period with and without a recipient (Ce^{3+} in the present instance). F_{DA} and F_D represent the donor's fluorescent strength in the existence and nonexistence of the recipient, accordingly. This suggests a partial transmission of STE production from the BaF_2 to Ce^{3+} in BaF_2-Ce. Thanks to its rapid degradation duration augmented by Ce integration, BaF_2-Ce would be desirable when it comes temporally strict measuring tasks and can be employed in the form of scintillating substance for tracking high-power granules such as β-beams as well as γ-beams. The rapid scintillating reaction can augment timing precision, a paramount factor when it comes to medicinal visualization. It is possible to utilize BaF_2-Ce within TOF-PET scanners for augmenting spatial visuals as well as lessening noise.

There have been limited researches of the scintillating characteristics of BaF_2-Ce [5], [6]. Additionally, there have not been studies on generating gamma photo-maximum with this type of scintillating material. The photo maximum within the gamma hue ranges indicates the starting point of the gamma generator. For gamma spectroscopy, the scintillator should create a light maximum with high power resolution. To investigate the use of BaF_2-Ce for gamma spectral analysis, we collected pulse height hue ranges from the radioisotopes. The pulse height hue range shows photo maxima at 511 keV, 662 keV, and 1274 keV. The power resolution of 13.5% at 662 keV has been determined employing the FWHM acquired from the Gaussian match of the entire power maximum region. The ceramic used was Ø 10×1 mm^2. For determining the scintillation illumination produced by BaF_2-Ce(0.2%) ceramic, the integrals of scintillation reaction were compared to those of NaI(Tl). A spectral revision element was applied, taking into account the spectrum emitting of BaF_2-Ce(0.2%), NaI(Tl), and PMT sensitivity. The luminosity produced by BaF_2-Ce(0.2%) is 5100 photons/MeV, which is equivalent to the 5000-7000 photons/MeV recorded for BaF_2-Ce sole crystal. BaF_2-Ce translucent ceramic is a cost-effective replacement to sole crystal scintillators due to its ability to generate photo-maxima, simplicity in production, and high mechanical durability. The lower cost can be attributed to various factors. When it comes to fabricating procedure, ceramics would be created via sintering powder samples with greater speed and smaller resource requirement while single crystal necessitates immaculate heat regulation, lengthy development durations, as well as costly apparatuses. When it comes to output and production scale, ceramic enables batch processing to facilitate concurrent fabrication for various samples while single crystal typically leads to small output because of faults, crevices as well as magnitude restrictions. It is possible to press and sinter ceramics to create quasi-net forms and limit waste while single crystals typically need machining posterior to growth, causing substance loss. In addition, it is easier to reglate the magnitude as well as shape BaF_2-Ce and this pliability proves highly desirable in huge-surface trackers and complicated geometrical forms. Ceramics can also withstand granular limits as well as small flaws, unlike single crystals that need to have almost no flaw for desirable proficiency. This quality lessens the requirement for strict quality regulation as well as rejectability. Based on an earlier study, BaF_2-Ce is capable of attaining identical scintillating illumination output as well as smaller postglimmer compared to single crystals, showing that proficiciency is preserved in spite of the smaller cost [27]. The desirable qualities of BaF_2-Ce, including rapid degradation duration as well as rapid scintillating reaction, can prove

helpful for various global fields, such as medicine, radiation detection, industrial systems, etc. The swift scintillating reaction as well as significant illumination output of BaF_2-Ce enables application to radioactivity scintillating interfaces in medicinal ausclation as well as examination in industries. Furthermore, with these qualities, the ceramic also proves proficient in tracking ionizing radioactivity throughout many power states, applicable to environment supervision, nuclear safety, as well as national security.

Figure 1 shows the link between particle size and light dispersion, with Figures 1(a)-(c) depicting the scattering coefficient, reduced scattering coefficient, angular scattering coefficient, respectively. It is possible to increase particle size through improved light transmission and wavelength conversion efficiency. Blue light brightness may increase when forward scattering and reabsorption decrease, but forward emission blue light dispersion increases. This is accomplished by increasing the particle size while lowering the concentration of yellow phosphorus. Similarly, the ability to select the appropriate color temperature (CCT) is limited. CCT is not concentration-dependent, as shown in Figures 2 and 3, however the dosage of YGA:Ce yellow phosphor increases with particle size, as seen in Figure 2. Increasing the particle sizes (16-20 μm), YGA:Ce phosphor ratios change (from about 27.20% to above 27.40%), as seen in Figure 2. Figure 3 depicts how increased doping reduces a phosphor's CCT variance. CCT values are highest at temperatures above 3050 K and particle sizes of around 16 μm.

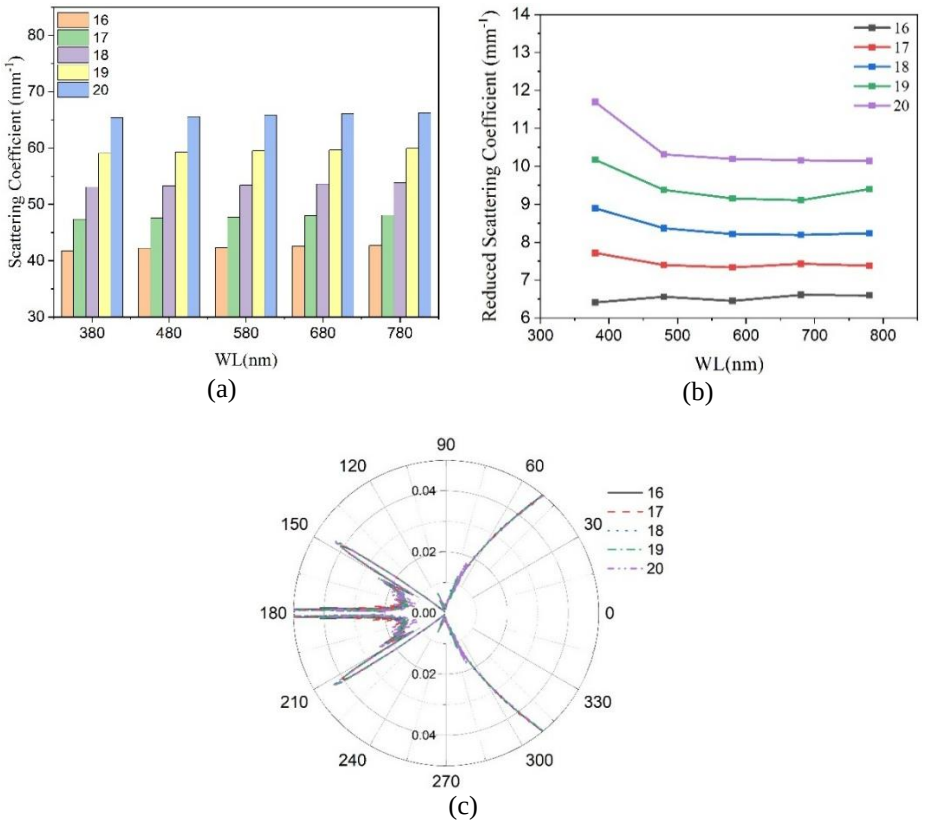

Figure 1. Scattering coefficients with various particle sizes (a) scattering coefficient, (b) reduced scattering coefficient, and (c) angular scattering coefficient

Figure 4 shows that particle size does not necessarily increase the brightness of white light emission. The highest results were obtained at particle size of 16 μm, while the lowest were obtained at particle size of 17 μm. Increased backscattering and reabsorption result in less blue emission and an uneven distribution of hues. When subjected to more backscattered blue light, increased particle sizes, for example, may cause the phosphor to shift from blue to yellow or orange-red. A specific particle size is required before the phosphor coating begins to expand. Because of the numerous reflections that the modified light would receive from various objects, the emission spectrum would be reduced. In other words, a high phosphor dose may increase the proportion of converted light that is back-reflected, which raises CCT while decreasing luminous intensity. Figure 5 shows how adding particle size of 16 μm to a simulated WLED with a lumen output power greater than 73.6 lm increases brightness and color uniformity.

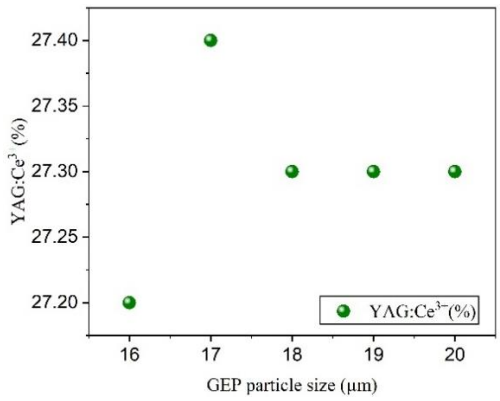

Figure 2. YGA:Ce phosphor proportion values with various particle sizes

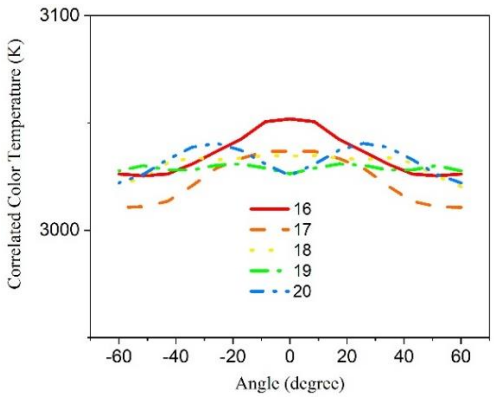

Figure 3. CCT values with various particle sizes

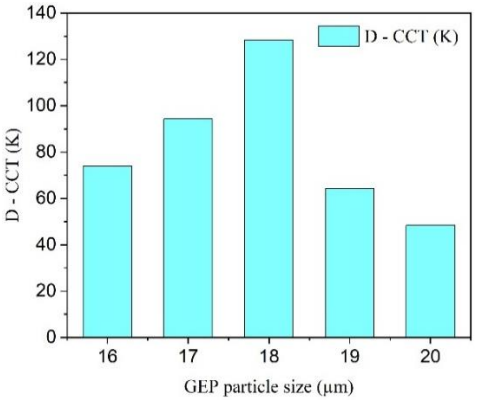

Figure 4. Color difference values with various particle sizes

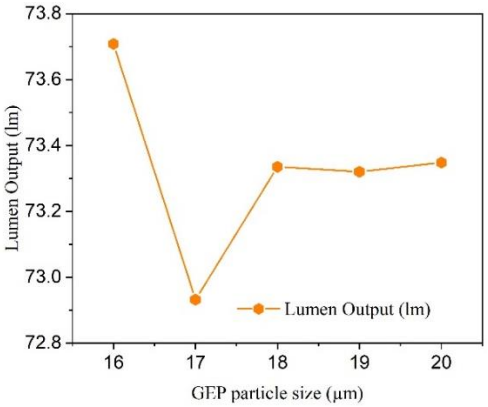

Figure 5. Luminescence strength with various particle sizes

The particle sizes have a significant impact on the brightness and hue rendition of white LEDs, as seen in Figures 6 and 7. Experiments with color rendition utilizing the color rendering indicator (CRI) and the color quality scale (CQS) revealed a consistent fluctuation as particle size increased to 20 μm. CRI and CQS declines could be attributed to the unpredictability of blue, green, and yellow-orange hues. High particle sizes result in irregular light emission with a bias toward the yellow-orange spectrum, as well as increased dispersion. We will adjust the CRI and CQS of this phosphor as we evaluate the results, as well as look into other factors like particle size.

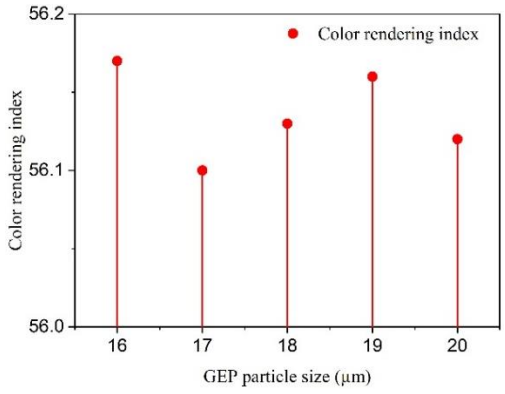

Figure 6. CRI values with various particle sizes

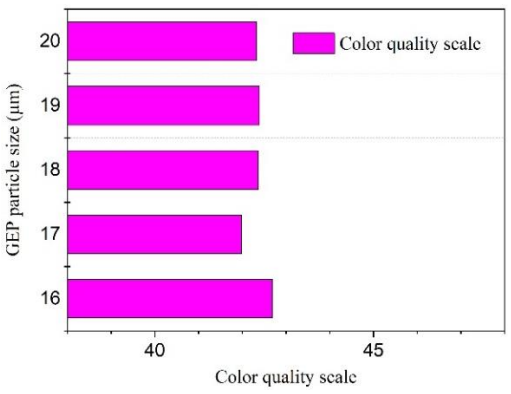

Figure 7. CQS values with various particle sizes

4. CONCLUSION

The illuminating and scintillation characteristics of a BaF_2-Ce(0.2%) translucent ceramic measuring Ø 10×1 mm^2 were investigated. The pulse height hue ranges of radioisotope Na-22 produced with BaF_2-Ce show photo maxima at 511 and 1274 keV, respectively. Cs-137's pulse height hue range exhibits a photo maximum at 662 keV. The FWHM measurement from a Gaussian fit of the whole power maximum region was used for calculating the 13.5% power resolution at 662 keV. The scintillation degradation measurements revealed a quick part of 58 ns for Ce^{3+} transformations and a more gradual part of 434 ns for dipole-dipole power transmission from the BaF_2 host network to Ce^{3+} luminous core. This indicates that the more slowly STE production in BaF_2 may have translated to the quicker Ce^{3+} luminosity. BaF_2-Ce(0.2%) exhibited comparable brightness and scintillating features when its sole crystal equivalent. Translucent ceramics offer benefits including inexpensive manufacturing costs, mechanical strength, and ease of manufacturing, making them a viable substitute for BaF_2-Ce sole crystal for scintillation purposes. BaF_2-Ce offer various qualities, including significant illumination output, rapid degradation duration, and rapid scintillating reaction, which are desirable for many global fields such as medicine, radiation detection, industrial systems and nuclear safety. Regardless, Ce is not necessarily the best dopant to create ceramics. Depending on needs and circumstances, other elements can be selected based on their distinctive qualities. For example, for acquiring a wider spectrum reaction, Eu, Sm, and Tb can be used to replace Ce, yielding strong red, orange-red, and green discharges, respectively. For neutron tracking as well as hybrid visualization, Gd may be a candidate for its significant neutron cross-section. Therefore, our future research effort may focus on other dopants for BaF_2 to cover different optical scenarios.

ACKNOWLEDGMENTS

The authors wish to express their gratitude to the Posts and Telecommunications Institute of Technology, Vietnam, for financial support for this research.

FUNDING INFORMATION

Authors state no funding involved.

AUTHOR CONTRIBUTIONS STATEMENT

This journal uses the Contributor Roles Taxonomy (CRediT) to recognize individual author contributions, reduce authorship disputes, and facilitate collaboration.

Name of Author	C	M	So	Va	Fo	I	R	D	O	E	Vi	Su	P	Fu
Luu Hong Quan	✓	✓	✓	✓	✓	✓	✓	✓	✓	✓	✓	✓	✓	
Nguyen Thi Phuong Loan		✓		✓		✓		✓	✓	✓	✓	✓		

C : **C**onceptualization
M : **M**ethodology
So : **So**ftware
Va : **Va**lidation
Fo : **Fo**rmal analysis
I : **I**nvestigation
R : **R**esources
D : **D**ata Curation
O : Writing - **O**riginal Draft
E : Writing - Review & **E**diting
Vi : **Vi**sualization
Su : **Su**pervision
P : **P**roject administration
Fu : **Fu**nding acquisition

CONFLICT OF INTEREST STATEMENT

Authors state no conflict of interest.

DATA AVAILABILITY

Data availability is not applicable to this paper as no new data were created or analyzed in this study.

REFERENCES

[1] N. D. Q. Anh, "Nano scattering particle: an approach to improve quality of the commercial led," *The University of Danang - Journal of Science and Technology*, pp. 53–57, Mar. 2024, doi: 10.31130/ud-jst.2024.614e.
[2] H. T. Tung, N. T. P. Loan, and N. D. Q. Anh, "The Enhancement Chromatic Uniformity and Illuminating Flux of WLEDs with

Dual-Layer Phosphorus Configuration," in *International Conference on Advanced Engineering Theory and Applications*, 2024, pp. 167–174, doi: 10.1007/978-981-99-8703-0_14.
[3] H. T. Tung, B. T. Minh, N. L. Thai, H. Y. Lee, and N. D. Q. Anh, "ZNO particles as scattering centers to optimize color production and lumen efficiencies of warm white LEDs," *Optoelectronics and Advanced Materials - Rapid Communications*, vol. 18, no. 5–6, pp. 283-288, May-Jun. 2024.
[4] P. H. Cong, L. X. Thuy, N. T. P. Loan, H. Y. Lee, and N. D. Q. Anh, "ZnO-doped yellow phosphor compound for enhancing phosphor-conversion layer's performance in white LEDs," *Optoelectronics and Advanced Materials - Rapid Communications*, vol. 18, pp. 389-395, 2024.
[5] P. X. Le, N. D. Q. Anh, and H. Y. Lee, "Regulating the white LED properties with different SiO_2 particle sizes," *Optoelectronics and Advanced Materials - Rapid Communications*, vol. 18, pp. 485-489, 2024.
[6] N. D. Q. Anh and H. Y. Lee, "Titanium dioxide in vanadate red phosphor compound for conventional white light emitting diodes," *Optoelectronics and Advanced Materials - Rapid Communications*, vol. 18, pp. 480-484, 2024.
[7] S. D. Alaruri, A. J. Brewington, M. A. Thomas, and J. A. Miller, "High-temperature remote thermometry using laser-induced fluorescence decay lifetime measurements of Y/sub 2/O/sub 3/:Eu and YAG:Tb thermographic phosphors," in *IEEE Transactions on Instrumentation and Measurement*, vol. 42, no. 3, pp. 735-739, Jun. 1993, doi: 10.1109/19.231599.
[8] D.-C. Chen, Z.-G. Liu, Z.-H. Deng, C. Wang, Y.-G. Cao, and Q.-L. Liu, "Optimization of light efficacy and angular color uniformity by hybrid phosphor particle size for white light-emitting diode," in *2013 10th China International Forum on Solid State Lighting (ChinaSSL)*, Beijing, 2013, pp. 95-99, doi: 10.1109/SSLCHINA.2013.7177322.
[9] E. Juntunen, O. Tapaninen, A. Sitomaniemi, and V. Heikkinen, "Effect of Phosphor Encapsulant on the Thermal Resistance of a High-Power COB LED Module," in *IEEE Transactions on Components, Packaging and Manufacturing Technology*, vol. 3, no. 7, pp. 1148-1154, Jul. 2013, doi: 10.1109/TCPMT.2013.2260796.
[10] C. -T. Li and Y. Li, "Color-Decoupled Photo Response Non-Uniformity for Digital Image Forensics," *IEEE Transactions on Circuits and Systems for Video Technology*, vol. 22, no. 2, pp. 260-271, Feb. 2012, doi: 10.1109/TCSVT.2011.2160750.
[11] L. Liu, X. Tan, D. Teng, M. Wu, and G. Wang, "Simultaneously Enhancing the Angular-Color Uniformity, Luminous Efficiency, and Reliability of White Light-Emitting Diodes by ZnO@SiO2 Modified Silicones," *IEEE Transactions on Components, Packaging and Manufacturing Technology*, vol. 5, no. 5, pp. 599-605, May 2015, doi: 10.1109/TCPMT.2015.2424981.
[12] M. -R. Shin, R. -r. Moon, J. -Y. Lee, and Y. -J. Kim, "Proposal and design of hybrid light guide plate for large-area LED display to improve illuminance and color uniformity," in *Technical Digest of the Eighteenth Microoptics Conference*, Tokyo, Japan, 2013, pp. 1-2.
[13] J. Zou, F. Han, Z. Zhang, H. Zheng, S. Liu, and S. Liu, "Fabrication of Phosphor Pillar Based on Electrohy-drodynamic for High Angular Color Uniformity of White Light-emitting Diodes," in *2018 19th International Conference on Electronic Packaging Technology (ICEPT)*, Shanghai, China, 2018, pp. 1421-1425, doi: 10.1109/ICEPT.2018.8480503.
[14] X. Lu, W. Wang, Z. Su, S. Liu, and H. Zheng, "Phosphor particle spatial patterning for high angular color uniformity LED packaging through selective curing and settling," in *2019 20th International Conference on Electronic Packaging Technology(ICEPT)*, Hong Kong, China, 2019, pp. 1-4, doi: 10.1109/ICEPT47577.2019.245234.
[15] L. T. T. My, N. L. Thai, T. M. Bui, H.-Y. Lee, and N. D. Q. Anh, "Phosphor conversion for WLEDs: YBO3: Ce3+, Tb3+ and its effects on the luminous intensity and chromatic properties of dual-layer WLED model," *Materials Science Poland*, vol. 40, no. 4, pp. 105–113, Dec. 2022, doi: 10.2478/msp-2022-0050.
[16] H. T. Tung, D. A. N. Thi, and N. D. Q. Anh, "The effects of Ca14Mg2(SiO4)8:Eu2+ phosphor on white light emission quality of LED-phosphor packages," *Bulletin of Electrical Engineering and Informatics*, vol. 12, no. 6, pp. 3388–3394, Dec. 2023, doi: 10.11591/eei.v12i6.4792.
[17] H. T. Tung, M. H. N. Thi, and N. D. Q. Anh, "Improved color uniformity in white Light-Emitting diodes using LILU(MOO4)2:SM3+ combined SIO2 composite," *International Journal of Technology*, vol. 15, no. 1, pp. 8-17, Jan. 2024, doi: 10.14716/ijtech.v15i1.6165.
[18] H. T. Tung, N. D. Q. Anh, and H. Y. Lee, "Impact of phosphor granule magnitudes as well as mass proportions on the luminous hue efficiency of a coated white light-emitting diode and one green phosphor film," *Optoelectronics and Advanced Materials - Rapid Communications*, vol. 18, no. 1–2, pp. 58–65, Feb. 2024
[19] N. T. P. Loan, N. D. Q. Anh, N. C. Trang, and H.-Y. Lee, "Better color distribution uniformity and higher luminous intensity for LED by using a three-layered remote phosphor structure," *Materials Science Poland*, vol. 40, no. 1, pp. 60–67, Mar. 2022, doi: 10.2478/msp-2022-0010.
[20] X. Kong, Z. Qiu, L. Wu, Y. Lei, and L. Chi, "Luminescence Properties of Green Phosphor $Ca_2Ga_2(Ge_{1-x}Si_x)O_7$:y%$Eu^{2+}$ and Application," *Materials*, vol. 16, no. 10, pp. 1-9, May 2023, doi: 10.3390/ma16103671.
[21] Y. Li *et al.*, "Ultrabroadband Visible–Near-Infrared Phosphor $CaY_2Mg_2Ge_3O_{12}$:Ce^{3+}/Cr^{3+} and its temperature sensing," *Inorganic Chemistry*, vol. 63, no. 50, pp. 23849-23857, Dec. 2024, doi: 10.1021/acs.inorgchem.4c04088.
[22] P. Ge *et al.*, "Upconverted persistent luminescent $Zn_3Ga_2SnO_8$: Cr^{3+}, Yb^{3+}, Er^{3+} phosphor for composite anti-counterfeiting ink," *Applied Optics*, vol. 61, no. 19, pp, 5681-5685, Jun. 2022, doi: 10.1364/ao.456302.
[23] A. Bashir, M. Ahmed, S. Aslam, and M. Ikram, "Low temperature UV assisted water based solution processing: investigation of structural, optical, and electrical characteristics of yttrium oxide thin films," *Semiconductor Science and Technology*, vol. 40, no. 5, p. 055009 Apr. 2025, doi: 10.1088/1361-6641/adca50.
[24] M. M. Damoom, A. M. Alhawsawi, E. Banoqitah, E. Moustafa, and A. H. Hammad, "Impact of TeO_2 on the structure, optical, and photoluminescence characteristics of BaO–V_2O_5–P_2O_5 vitreous materials," *Physica Scripta*, vol. 100, no. 4, p. 045956, Mar. 2025, doi: 10.1088/1402-4896/adc167.
[25] S. R. Bhelave, A. N. Yerpude, and S. J. Dhoble, "Photoluminescence studies and optimistic applications of KAlSiO4 phosphor synthesized by combustion method," *Journal of Optics*, Aug. 2024, pp. 1-12, doi: 10.1007/s12596-024-02021-7.
[26] Y. Kuang, W. Chen, Y. Wang, Y. Sun, J. Jin, and Z. Xia, "Narrow-band green/red-emitting glass composites enabling highly stable patterned wheel for laser phosphor display," *Science China Materials*, vol. 68, no. 6, pp. 1822–1829, May 2025, doi: 10.1007/s40843-025-3361-1.
[27] X. Lv, Y. Liang, Y. Zhang, D. Chen, X. Shan, and X.-J. Wang, "Deep-trap ultraviolet persistent phosphor for advanced optical storage application in bright environments," *Light Science & Applications*, vol. 13, no. 1, Sep. 2024, doi: 10.1038/s41377-024-01533-y.

BIOGRAPHIES OF AUTHORS

Luu Hong Quan received the degree in Electrical Engineering from Ho Chi Minh City University of Technical Education, Vietnam, in 1998; an M.Sc. in Power Plant and Network Equipment from Ho Chi Minh City, Vietnam, in 2009; and a Ph.D. degree of Doctor of Philosophy in Control Engineering and Automation from Hanoi University of Mining and Geology, in 2023. He is a currently working at the University of Industry and Trade, Ho Chi Minh City, Vietnam. His research interests include renewable energy, control engineering, and automation. He can be contacted at email: quanlh@huit.edu.vn.

Nguyen Thi Phuong Loan was born in Da Nang Province. In 2006, she received her master degree from University of Natural Sciences. Her research interest is optoelectronics. She has worked at the Faculty of Fundamental 2, Posts and Telecommunications Institute of Technology, Ho Chi Minh City, Vietnam. She can be contacted at email: ntploan@ptithcm.edu.vn and nguyenthiphuongloan8899@gmail.com.